Journal of
Synchrotron
Radiation

ISSN 1600-5775

Received 15 February 2014
Accepted 22 May 2014

The Sirius project

Lin Liu,* Natalia Milas, Afonso H. C. Mukai, Ximenes R. Resende and Fernando H. de Sá

Brazilian Synchrotron Light Laboratory (LNLS), Campinas, SP, Brazil. *E-mail: liu@lnls.br

The lattice design and beam dynamics optimization for Sirius, a new low-emittance synchrotron light source presently under construction at the Brazilian Synchrotron Light Laboratory (LNLS) in Campinas, Brazil, is presented. The electron storage ring is based on a five-bend achromat (5BA) design achieving a bare lattice emittance of 0.28 nm rad for a 3 GeV beam. The circumference of 518 m contains 20 achromatic straight sections of alternating 7 m and 6 m in length. An innovative approach is adopted to enhance the performance of the storage ring dipoles by combining low-field (0.58 T) magnets for the main beam deflection with a very short 2 T permanent-magnet superbend sandwiched in the center dipole. This superbend creates 12 keV critical photon energy dipole sources with modest total energy loss from dipoles. In addition it also creates a longitudinal dipole field gradient that reduces the emittance by about 10%. The optimized dynamic aperture allows for top-up operation with off-axis injection and the optimized energy acceptance allows for a total beam lifetime of around 11 h at nominal current with a third-harmonic cavity.

Keywords: multi-bend achromat; superbend; diffraction-limited storage ring.

1. Introduction

The Sirius project was proposed and designed to meet the growing demand for high-brightness synchrotron radiation in Brazil. Since 1997, when LNLS completed construction and opened the first synchrotron light facility in the southern hemisphere, a 1.37 GeV light source known as UVX, the users community in Brazil has grown and matured. In 2013 a total of 1163 researchers had carried out 395 experiments at the 18 UVX beamlines. Along over more than 16 years of routine operation for users, the expansion capabilities for this light source, either in terms of new beamlines or upgrades to its accelerators, have reached fundamental limits that can no longer be overcome. Clearly, in order to keep the competitiveness of the Brazilian scientific community in the future, it is fundamental that a source with orders-of-magnitude increase in photon flux and brightness be provided, one that will enable state-of-the-art techniques for exploring transverse coherence and nano-focusing applications in the soft and hard X-ray ranges. The first discussions about a new low-emittance light source for Brazil started in 2006 among the scientific and accelerator communities, during the 16th LNLS Annual Users Meeting. In November 2008 a decision by the Brazilian Federal Government was taken to fund preliminary studies for this new source, leading to the final decision to approve the project in 2011. In the meantime, as several different types of magnetic lattices were studied for Sirius and prototype work for the main subsystems started, worldwide explorations towards building diffraction-limited storage rings (DLSRs) began to evolve, driven by recent developments in accelerator technology. While diffraction-limited rings in the hard X-ray energy range still have R&D challenges to face even today, MAX IV, a soft X-ray DLSR with emittance as low as 0.33 nm rad (Leemann *et al.*, 2009), achieved with a seven-bend achromat lattice, started construction in 2011. In June 2012, incited by the Machine Advisory Committee, Sirius joined MAX IV in this class of medium-energy medium-size soft X-ray DLSRs, by designing a five-bend achromat lattice with 0.28 nm rad emittance at 3 GeV. One feature from the early designs that was kept in the new machine is the use of low-field bend magnets with a high-field 2 T slice superbend in the center dipole. In this way hard X-ray dipole radiation is produced only at the beamline exit, preserving the benefits of low overall dipole radiation power. Fig. 1 shows the brightness achieved in Sirius with small-gap in-vacuum undulators, elliptically polarizing undulators (EPUs) in linear polarization mode, wigglers and 2 T superbends, where the effects of insertion devices (IDs) and intrabeam scattering blow-up on the emittance and energy spread of the electron beam are taken into account.

The Sirius project is already under construction and will be situated in the same LNLS campus, close to the present UVX light source. Fig. 2 shows an aerial view of the campus with the site where Sirius is being built.

In this paper we describe the performance parameters expected for Sirius resulting from the optics and nonlinear beam dynamics optimization of the lattice achieved up to date.

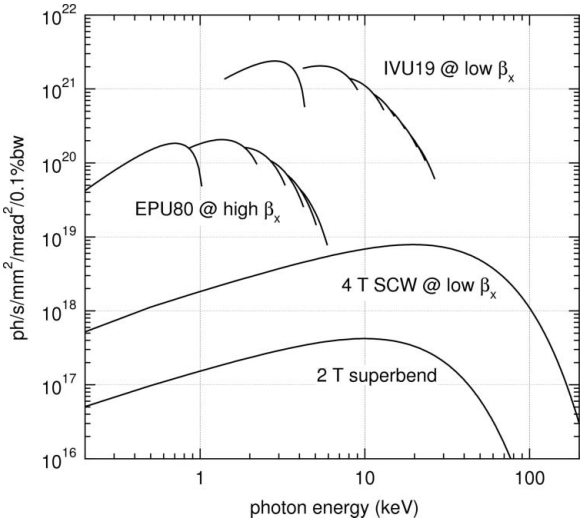

Figure 1
Brightness of the Sirius radiation sources including effects of insertion devices and intrabeam scattering on emittance and energy spread for 500 mA total beam current. IVU19: hard X-ray in-vacuum undulator with 19 mm period and 4.5 mm magnet gap. Odd harmonics up to 15th are plotted. 4 T SCW: 4 T superconducting wiggler presently operating in UVX. EPU80: elliptically polarizing undulator with 80 mm period in planar phase. Calculations performed with *SRW* (Chubar & Elleaume, 1998).

The key ingredient to increase the brightness of a synchrotron light source is the electron beam emittance, a measure of the size and divergence of the beam. The natural equilibrium emittance is determined by the balance of radiation damping and quantum excitation of the particle oscillations, and depends only on the magnet lattice parameters. One of the most effective techniques to reduce the emittance is to increase the number of dipoles in the lattice cell, or achromat, to keep the dispersion function limited to small values in the bends. This is known as the multi-bend achromat (MBA) approach. The small dispersion requires strong focusing quadrupoles that, in turn, require strong sextupoles to compensate for the chromatic aberrations introduced. The sextupoles introduce strong nonlinearities in the beam dynamics, reducing the stable regions in phase space for the particles. Moreover, to achieve the strong quadrupole and sextupole strengths, small bore radii have to be used, leading to small apertures for the vacuum chamber. This implies not only technical difficulties for vacuum pumping and radiation heat extraction, but also increases the overall beam impedance and related effects. The strong magnets also lead to tight tolerances for field quality, alignment and excitation errors. Even though the MBA lattice approach is well known, the difficulties described above hampered concrete implementation of storage-ring projects based on MBA lattices. However, recent developments in accelerator technology have encouraged the first teams, including the Sirius team, to propose the use of MBA lattices as the basis for concrete storage-ring projects.

Figure 2
Aerial view of the LNLS campus in Campinas, Brazil, with the new light source Sirius drawn on the picture. The present light source UVX is located inside the largest square building.

2. Lattice design and basic beam parameters

Several different types of magnetic lattices have been studied for Sirius over the past few years. The choice is a 20-cell five-bend achromat (5BA) with natural emittance of 0.28 nm rad at 3 GeV. The circumference is 518.4 m and there are 20 dispersion-free straight sections for insertion devices and machine utilities. Among many lattices studied, this one showed the best compromise in terms of low emittance and large number of ID straight sections for a given constraint in the ring circumference. In addition, the lattice nonlinear optics was optimized to a sufficiently large dynamic aperture and momentum acceptance, allowing for conventional off-axis injection and large beam lifetime of about 7 h with realistic error tolerances and ID effects.

The low emittance is mainly achieved with the MBA approach, with M equal to 5. However, besides the number of dipoles, other parameters have also been optimized to reduce the emittance: (*a*) a transverse field gradient is added to the dipoles to increase the horizontal damping partition number as well as to match the optics, (*b*) a low bending field and achromatic conditions in the straight sections are used to enhance the effect of IDs on emittance reduction, (*c*) different dipole lengths in the cell are used to minimize the contribution of the end dipoles to the emittance, since the dispersion function at the achromat ends is matched to the zero-dispersion condition and not to the minimum emittance condition, and (*d*) a simple longitudinal field gradient is introduced in the center dipole, created by sandwiching a thin high-field permanent-magnet dipole of 2 T between two low-field dipoles of 0.58 T. The use of longitudinal dipole gradients to reduce the emittance has been discussed by many authors (see, for example, Nagaoka & Wrulich, 2007; Wang, 2009) and the idea is to design the dipole field and the optical functions so that the radiated energy is higher at places where the damping is larger than the excitation rate. For Sirius, the optics is designed so that the center of the achromat is the optimum position to place a strong dipole field. In addition to reducing

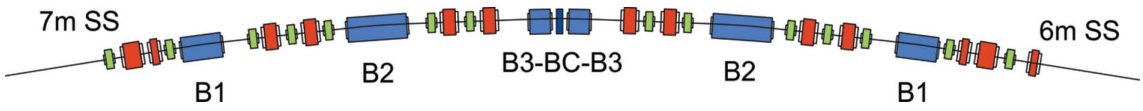

Figure 3
Layout of the modified 5BA arc showing the high-field 2 T thin dipole BC sandwiched in the center dipole B3–BC–B3. Also shown are the two types of straight sections, 7 m and 6 m in length. Quadrupoles are represented in red and sextupoles in green.

Table 1
Sirius main parameters.

Energy	3.0	GeV
Nominal current	350	mA
Circumference	518.4	m
Straight sections, number × length	10 × 7 m; 10 × 6 m	
Betatron tunes, horizontal/vertical	46.18/14.15	
Natural chromaticity, horizontal/vertical	−113/−80	
Horizontal natural emittance (bare)	0.28	nm rad
Vertical natural emittance (at 1% coupling)	2.8	pm rad
Natural bunch length	2.6 (8.8)	mm (ps)
Beam size at 1% coupling, no IDs		
7 m straight section	68.3 × 3.0	μm
6 m straight section	33.5 × 1.4	μm
Center of superbend (BC)	11.0 × 4.0	μm

the emittance by about 10%, these thin high-field dipoles will also produce hard X-rays of critical photon energy of 12 keV, and thus usable flux up to about 50 keV, in just a small horizontal angular fan, keeping the overall dipole radiation power at a low level. The option for a relatively low dipole field also favors a smaller beam energy spread.

Fig. 3 shows a schematic drawing of one Sirius 5BA achromatic cell with the high-field thin dipole BC sandwiched in the center dipole B3–BC–B3. The total deflection per cell is 18°, composed of the deflections of 2.77°, 4.10° and 4.26°, respectively, by B1, B2 and the set B3–BC–B3. The two types of straight sections are shown to the left (7 m) and right (6 m).

The lattice has alternating high and low horizontal betatron functions in the straight sections for insertion devices. A quadrupole doublet is used to match the high-β sections while a triplet is used in the low-β ones. This variation results in different free lengths for insertions in the straight sections, 7 m and 6 m, for otherwise identical straights. The vertical betatron function in the straight sections is always low to minimize the impact of the insertion devices on the optics. The high-β sections are better suited for the cases where a small electron beam divergence is important, whereas the low-β ones are recommended for the cases where a small beam size is favored. The optical functions are shown in Fig. 4.

In the arc sections the dispersion function reaches a maximum of 8 cm. A pair of quadrupoles between the dipoles is used to focus the beam in the horizontal plane whereas in the vertical plane only the dipole field gradient and edge focusing are used.

The main parameters of the Sirius storage ring are shown in Table 1.

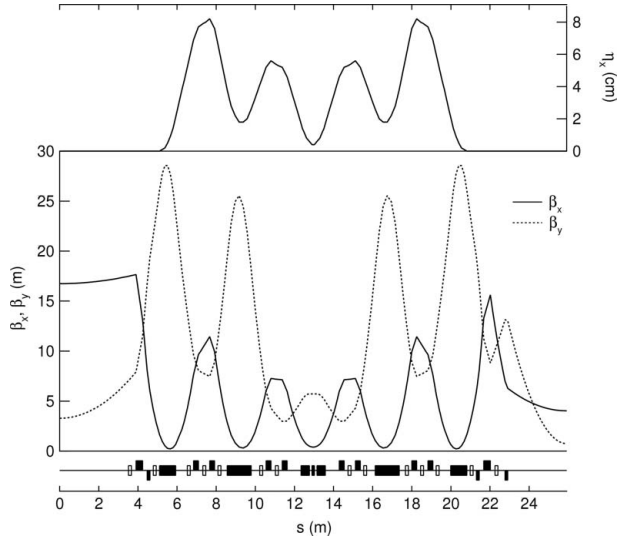

Figure 4
Lattice functions for one half of a 5BA period. The full superperiod consists of this cell reflected about either ID straight section center: high horizontal β, 7 m long on the left or low horizontal β, 6 m long on the right.

3. Operation scenarios for Sirius

In this section the operation scenarios for Sirius from commissioning to maximum current and full insertion devices usage are described. The parameters for each phase, shown in Table 2, will be used in the following sections to estimate beam lifetime and instability thresholds and also to make an assessment of the operation conditions of the storage ring.

In the commissioning phase (Phase 0) the energy loss is due only to dipoles and no insertion device is restricting the vertical acceptance of the machine. The RF voltage is provided by three normal-conducting cavities (NC) and the

Table 2
Sirius scenarios for beam lifetime and instability threshold calculations.

	Phase 0 Commissioning	Phase 1 Initial user mode	Phase 2 Final user mode	
Maximum total current	100	100	500	mA
Current/bunch (uniform fill)	0.116	0.116	0.579	mA
Single bunch current	–	–	2	mA
RF cavities	3 NC	3 NC	6 NC + HC	
Natural emittance†	0.28	0.22	0.19	nm rad
Coupling	1	1	1	%
IDs	–	6 IVUs, 4 EPUs, 1 SCW	12 IVUs, 8 EPUs, 1 SCW	
Natural energy spread†	0.083	0.093	0.091	%
Natural bunch length†	3.2	3.7	12.7	mm

† 'Natural' here refers to values for zero current. The effects of insertion devices and harmonic cavity are included.

maximum stored current is 100 mA, distributed in a uniform-filling pattern.

In the initial users mode (Phase 1), the first 13 beamlines described in the next section are included. The IDs for these beamlines include four in-vacuum undulators with 4.5 mm minimum gap (IVU19), two in-vacuum undulators with 8.0 mm minimum gap (IVU25), four EPUs and one superconducting wiggler (SCW) transferred from the present storage ring (UVX). All those insertion devices add about 200 keV to the energy loss/turn and cause a reduction in the natural emittance from 0.28 to 0.22 nm rad. The same RF cavities and stored current of the commissioning phase are assumed.

Table 3
Parameters for the Sirius 13 first beamlines (Phase 1).

Beamline	Technique	Source	Energy range
CARNAÚBA	Nano-diffraction	IVU19, gap = 4.5 mm	2–24 keV
EMA	Micro-XAFS	IVU19, gap = 4.5 mm	2–24 keV
INGÁ	Inelastic X-ray scattering	2 × IVU25, gap = 8 mm	5–24 keV
CATERETÊ	Coherent SAXS	IVU19, gap = 4.5 mm	2–24 keV
MANACÁ	Protein crystallography	IVU19, gap = 4.5 mm	2–24 keV
IPÊ	Inelastic soft X-ray scattering	2 × EPU80	10–2000 eV
SABIÁ	Soft X-ray spectroscopy	2 × EPU80	200–2000 eV
IMBUIA	Infrared aSNOM	Bending magnet edge	0.001–1 eV
JATOBÁ	High-energy tomography	4 T SCW	30–200 keV
MOGNO	Tomography, XPD/PDF	2 T superbend	4–24 keV
QUATI	Quick EXAFS	2 T superbend	4–45 keV
SAPUCAIA	SAXS	2 T superbend	4–24 keV
PAINEIRA	XPD	2 T superbend	4–45 keV

The IDs for the final scenario (Phase 2) are not defined yet and it is therefore more difficult to estimate their impact on the beam parameters. It was then considered the doubling of the number of IVUs and EPUs, adding 150 keV to the energy loss/turn. For the purpose of lifetime estimation and machine subsystems design, such as vacuum and RF, a maximum current of 500 mA is being considered. In this case, to have a reasonable lifetime, it is necessary either to install three additional normal-conducting cavities or exchange the whole system with two superconducting ones. A third-harmonic cavity (3HC) is also necessary to flatten the potential in the RF bucket. This is essential both to increase the bunch length and the synchrotron tune spread. The former improves beam lifetime by reducing the charge density, and the latter increases beam stability by adding Landau damping. A factor of about five increase in bunch length can be achieved for a uniform bunch filling pattern.

4. Insertion devices and effects on equilibrium parameters

An initial set of 13 beamlines (Phase 1) is planned for Sirius that cover all conventional techniques existing today at LNLS using the 2 T superbends, and also provide state-of-the-art techniques that explore coherence, micro- and nano-focusing and high energies using a total of 11 insertion devices. The parameters for the Phase 1 beamlines are shown in Table 3.

The effects of these 11 insertion devices on the beam equilibrium emittance and energy spread are shown in Fig. 5. The effect of a hypothetical set of Phase 2 insertion devices, where the Phase 1 devices are doubled with the exception of the SCW, is also shown in Fig. 5.

5. Error tolerance specifications and optics correction

When built, the storage ring will inevitably have errors in its magnets, be it in their construction or alignment in the tunnel. Moreover, intrinsic perturbations such as ground vibrations and ripple in the power supplies of the magnets have to be taken into account for proper parameter specification and beam quality control.

Alignment and field excitation errors in magnets will lead to beam dynamics distortions that, even if compensated by orbit and tune correction systems, may severely degrade the injection process or the stability of the stored beam. Based on statistical tracking simulations, where the errors are properly modeled, tolerances for positioning of the magnet centers in both planes, rotation about the longitudinal axis and field strength errors are determined for Sirius. A value of 40 μm for misalignment of the magnets is tolerable, whereas 0.2 mrad for roll rotation error and 0.05% excitation errors are also acceptable values. These are very tight tolerances that require not only state-of-the-art instrumentation and techniques but also innovative solutions for magnet design, production and installation. Two closed-orbit correction systems are designed for Sirius, the slow (SOFB) and fast (FOFB) orbit feedback systems. They will rely on orbit readouts of 200 beam position monitors distributed along the ring and on 160 horizontal and 120 vertical slow dipolar correctors plus 80 fast correctors in each plane. These numbers are adequate to effectively mini-

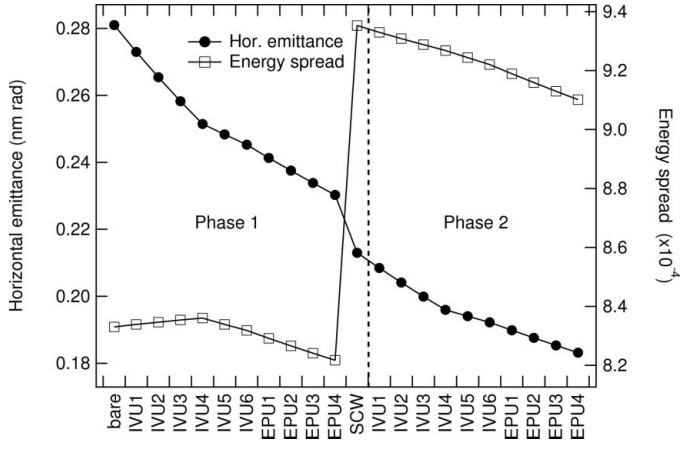

Figure 5
Effect of insertion devices on the Sirius natural emittance and energy spread. To the left, the effects of Phase-1 IDs for the first 13 beamlines are considered (six IVUs, four EPUs and one SCW). To the right, a hypothetical scenario with twice the number of IVUs and EPUs is considered. The big jump in emittance and energy spread is due to a 4 T superconducting wiggler.

mize orbit distortions in a large frequency range, from the slow temperature drifts to the fast variations caused by ID movements, and thus meet the required stability of beam position delivered to the beamlines.

Each orbit feedback system is optimized for operation under certain conditions. While the SOFB system is adequate for low bandwidth and strong corrections, the FOFB system has high bandwidth but can only handle weak corrections. In practice there will be perturbations that cannot be effectively attenuated by either system, especially those with frequencies above 1 kHz. The amplitudes of these perturbations have thus to be limited so that their effect on the beam should be smaller than 10% of the original beam size. A tolerance of 20 p.p.m. for ripple in the dipole and quadrupole power supplies and a 6 nm tolerance for the residual r.m.s. vibration amplitude of these magnets (after SOFB and FOFB corrections) integrated in all frequencies have been defined.

Undesirable nonlinear fields from magnets are also detrimental to the beam, reducing the dynamic and momentum apertures. To take this effect into account, nonlinear magnetic fields (multipoles) from three-dimensional models of the magnets are input into ring simulations. A set of acceptable tolerances for field multipoles has also been defined for all dipoles, quadrupoles and sextupoles. Nonlinear fields for insertion devices were simulated as well using kick tables.

Another consequence of the alignment and rotation errors is the coupling between the vertical and horizontal electron trajectories, leading to a large equilibrium vertical beam size that would otherwise be practically zero. In order to minimize this effect, a coupling correction system has also been devised for Sirius. It is composed of 40 independently excited skew quadrupoles whose fields are implemented as additional pole-winding coils in one of the sextupole families. With such a correction system, the coupling, defined as the ratio between vertical and horizontal emittances, can be controlled to the 0.1% level. Ultimately, for beam lifetime purposes, the vertical beam size will be set to an equivalent 1% coupling level.

Excitation errors of quadrupoles and off-center beam closed-orbits at sextupoles break the symmetry of the linear optics and alter betatron phase advances. These effects spoil the sextupole configuration achieved while optimizing the nonlinear dynamics of the ring without errors (see next section). In order to restore the original beam stability, optics symmetrization can be performed in the ring, consisting of fine tuning each quadrupole field until the measured optics approaches the original one (Safranek *et al.*, 2002). This procedure, together with the others described previously, can mitigate much of the negative impact of lattice errors on beam properties.

6. Nonlinear beam dynamics

The strong nonlinear magnetic fields required to lower the beam emittance lead to a reduced volume in phase space where the particles are stable, or reduced dynamic and momentum apertures. The nonlinear optimization consists of attempting to increase these apertures by changing the phase advance per cell and minimizing the amplitude- and momentum-dependent effects on the particle dynamics, mitigating the effects of nonlinear resonances. For beam injection and accumulation, the dynamic aperture has to accommodate the stored beam, the injected beam and the septum wall thickness. For Sirius, with some safety margin, the target dynamic aperture to assure a high-efficiency injection process is set to about 8 mm in the inner horizontal side of the ring at the injection section. A good beam lifetime is achieved when the average momentum aperture along the ring is larger than $\pm 4\%$.

The nonlinear optimization approach used for Sirius can be divided into several stages. Initially, many iterations between linear and nonlinear optics are necessary to adjust the optical functions in such a way as to create good locations for sextupoles, minimize the natural chromaticity of the ring and tune the cell to reduce resonance driving terms and tune shifts with amplitude. The optimization was subject to various constraints such as the small ring emittance, the total circumference of the machine, the minimum distances between elements, the maximum strength for magnets and the required betatron functions at the ID straight sections. Once good initial results were obtained with this first optimization step, the magnets position, number and maximum strengths were frozen, significantly reducing the number of variables of the problem.

In a second stage, basically the tunes and the configuration of nine sextupole families are varied to optimize the dynamic aperture and momentum acceptance calculated by numerical tracking. This is a very time-consuming process and we resort to a multiobjective optimization code using a genetic algorithm solver, *MOGA* (Borland *et al.*, 2010) which uses *Elegant* (Borland, 2000) as tracking code. *MOGA* runs result in a set of solutions, each of which tries to satisfy two objectives at an acceptable level, the dynamic aperture at injection and the momentum acceptance (or Touschek lifetime), without one being dominated by the other. All sextupole and quadrupole families are used as limited variables that have to satisfy strong constraints imposed on the lattice optics, such as the symmetry properties, the limited range of variation for the phase advances and betatron function values, *etc*. The results are then tested against an ensemble of machines with IDs, physical limitations and realistic errors (see previous section on lattice errors). This process involves the generation of several models of the storage ring with different seeds for random alignment, excitation and multipole errors in all magnets, followed by correction of the orbit and tunes of each machine, simulating algorithms that will eventually be implemented in the real machine. Based on the results of these tests, the solution can be iterated again or not. The optimization process is continually updated based on new data as they become available from prototype magnetic measurements.

Figs. 6(*a*) and 6(*b*) show the dynamic and momentum apertures for 12 machines with all IDs considered for Phase 2 (EPUs in horizontal polarization mode), physical limitations, random alignment, excitation and multipole errors and orbit and tune correction. It is possible to notice that the vacuum

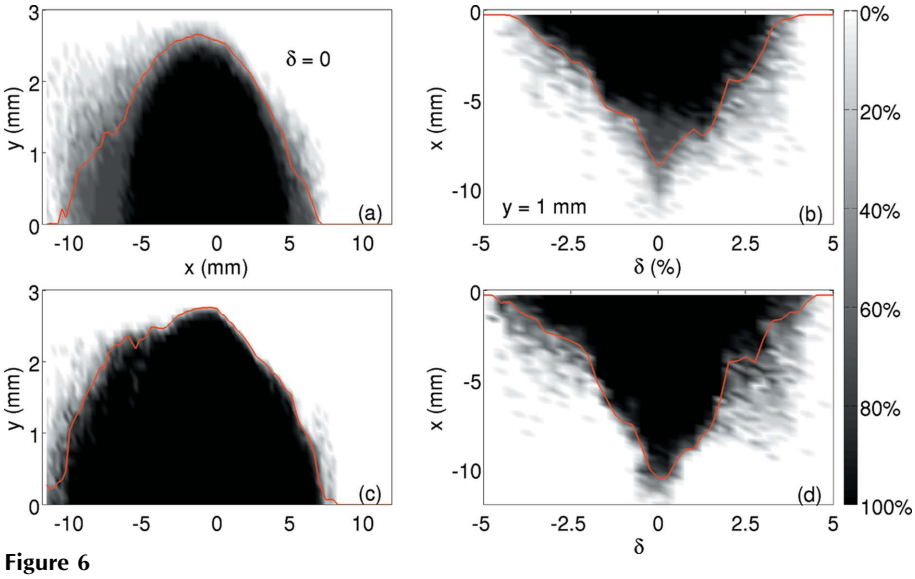

Figure 6
Dynamic (left) and momentum (right) apertures at the center of the 7 m straight section for 12 machines with random alignment and multipole errors, orbit and tune corrections (top and bottom) and additional coupling and beta-beating corrections (bottom). The gray scale represents the percentage of simulated machines for which a given point of the grid represents a stable condition. Red curves represent average apertures. For these calculations, the following configuration was used: six-dimensional tracking; dynamic apertures are calculated for on-momentum particles for 5000 turns; momentum apertures are calculated for y = 1 mm for 3500 turns; a constant physical aperture of 12 mm × 12 mm is considered along the ring; IDs from Table 3 are considered (EPUs in horizontal polarization).

chambers are not limiting the dynamic aperture, which means that we still have room for improvement. However, the negative horizontal aperture, which is the relevant parameter for beam injection, is already approaching the physical aperture.

The EPUs were also simulated in other polarization modes but their intrinsic magnetic field roll-offs introduce unacceptable dynamic aperture reductions. Active compensation of field roll-offs and novel EPU designs are being considered to avoid this problem.

As discussed in previous sections, other correction schemes, such as coupling and symmetrization, are being studied for further dynamic and momentum aperture improvement. Figs. 6(*c*) and 6(*d*) show the apertures of the same machines as Figs. 6(*a*) and 6(*b*) with additional coupling correction and symmetrization of the linear optics. Before correction, coupling has an average value of 12%, dropping down to 0.1% after correction. Beta-beating before symmetrization has a standard deviation of approximately 5% and 10% in the horizontal and vertical planes, respectively. Symmetrization can completely suppress beta-beating in the simulations. Overall, the effect of these corrections is a significant increase in the stable region for all the simulated machines. However, the applicability of these corrections in the real machine, with the precision achieved in simulations, is still uncertain and, in addition, requires an already stable beam; for these reasons, they are considered as possible future upgrades for Sirius operation. The dynamic and momentum apertures obtained without the corrections are already large enough for the commissioning phase and initial users operation mode.

7. Collective effects and lifetime

To increase the brightness of synchrotron light sources, not only is the emittance progressively reduced, but also high beam intensities are used. As the intensity of the electron beam increases, the electromagnetic fields generated by the beam itself interact with the various elements of the vacuum chamber and may lead to instabilities. It is therefore important to study these collective effects. Furthermore, the increased charge density affects the interaction among electrons within the bunches, contributing to the values of equilibrium beam emittances and lifetime through intrabeam scattering and Touschek effect.

7.1. Impedance budget and instabilities

The beam–environment interaction can be described by the impedance concept, where each structure is modeled by a frequency-dependent complex function. The Sirius impedance budget may be divided into two types: the resistive wall impedances and the geometric impedances. The first kind was estimated using analytical formulae (Mounet & Metral, 2009) and the second with the help of numerical codes. So far, the resistive part of the impedance was calculated for the main components of the ring and the geometric part is represented by a broadband model based on the results of similar projects.

With the impedance budget, collective instability thresholds for Sirius have been calculated for the various operation scenarios described before, for coupled-bunch and single-bunch effects. Regarding coupled-bunch instabilities, the resistive wall instability for Phase 1 will have a growth rate of approximately a factor four greater than the damping rate at zero chromaticity. By increasing the chromaticity there is a strong head–tail damping of the azimuthal mode zero, and at a normalized chromaticity of only 0.03 (horizontal) and 0.06 (vertical) all modes are stable. However, this behavior depends strongly on the strength of the broadband impedance and, for the sake of safety, a transverse feedback system will be installed in the machine from the beginning. For Phase 2 the conclusions are the same as for Phase 1 with the growth rates around 20 times the machine damping rate for zero chromaticity.

Table 4 shows the current thresholds for single-bunch instabilities, where mode coupling is the most severe limiting effect. In Phase 1, the storage ring will be operated with 0.12 mA per bunch, which is well below the thresholds calculated for all three planes. For Phase 2, because of the third harmonic cavity, the bunches will no longer be Gaussian, and this breaks the assumptions made in the theoretical

Table 4
Current threshold for single-bunch instabilities in Sirius.

	Current threshold (mA)	
Mode coupling	Phase 1	Phase 2
Vertical	1.0	1.5
Horizontal	1.5	2.2
Longitudinal	2.1	$\gg 4$

models we have used for instability calculations (Cai, 2011; Chin, 1985). However, the operational current per bunch for this phase is still well below the calculated thresholds, resulting in a large safety margin.

As discussed in the next section, a hybrid filling pattern with an empty gap and a high-current single bunch for time-resolved experiments is planned for Sirius. In this mode the bunch lengthening provided by the harmonic cavity can be smaller and non-uniform. For the single bunch in the middle of the gap, even with optimum lengthening, the threshold current for mode coupling (see Table 4, Phase 2) is already below the nominal value of 2 mA. A tracking code that includes the effects of the harmonic cavity with uniform and non-uniform filling as well as broadband impedances is being developed to study the hybrid filling mode more carefully.

7.2. IBS and microwave instability

For a high-brightness beam it is important to calculate the impact of intrabeam scattering (IBS) and longitudinal mode coupling instability, also known as microwave instability, on the equilibrium beam parameters, since they can spoil the emittance and the storage ring performance. Both effects can be harmful especially when operating in a hybrid fill mode, where a high-current single-bunch is filled in the center of a small gap of empty buckets (about 5 to 10% of the total circumference), for time-resolved experiments. Table 5 shows the results for all operation scenarios and Fig. 7 shows the effect of the third-harmonic cavity on the equilibrium parameters as a function of single-bunch current for Phase 2.

7.3. Stored beam lifetime

The beam lifetime is also a key performance parameter for a light source. Various processes can lead to the loss of electrons from the beam; the most important ones are the collisions with residual gas molecules (gas scattering lifetime) and between two electrons with large momentum transfer (Touschek lifetime). Given the very low emittance of the machine, care has been taken to include IBS and microwave instability effects in the calculations. Concerning Touschek lifetime, it is import to note that the natural emittance of Sirius is already in the regime where there is an exponential increase in Touschek lifetime towards lower emittances, as can be seen in Fig. 8. From the plot it is clear that the inclusion of IDs in the machine, further reducing the emittance, is beneficial for the lifetime. In this regime the lifetime also shows a strong dependence on the energy acceptance. It is thus very important to optimize the lattice to have the largest possible energy acceptance.

Table 5
IBS effects on the equilibrium emittances for different operation conditions.

Scenario		ε_x (nm rad)	ε_y (pm rad)	σ_δ (%)	σ_s (mm)
Phase 0†	Zero current	0.28	2.8	0.083	3.2
	100 mA	0.30	3.0	0.091	3.5
Phase 1	Zero current	0.22	2.2	0.093	3.7
	100 mA	0.23	2.3	0.099	3.9
Phase 2	Zero current	0.19	1.9	0.091	12.7
	500 mA	0.21	2.0	0.098	13.2
	2 mA/bunch	0.26	2.2	0.109	13.9

† Commissioning.

Table 6 shows results from lifetime calculations for uniform fill for different scenarios. For all cases the total lifetime is between 8 and 11 h. For Sirius there are users also interested in time-resolved experiments and thus an estimate for single-bunch lifetime is needed. Calculations of lifetime for a single bunch of 2 mA (3.6 nC) were performed using parameters from Phase 2 and are also included in Table 6.

8. Conclusions

The lattice design and beam dynamics optimization for Sirius, a new synchrotron light source under construction in Brazil, that will be diffraction-limited in the soft X-ray energy range, was presented. Calculations show that the designed machine is

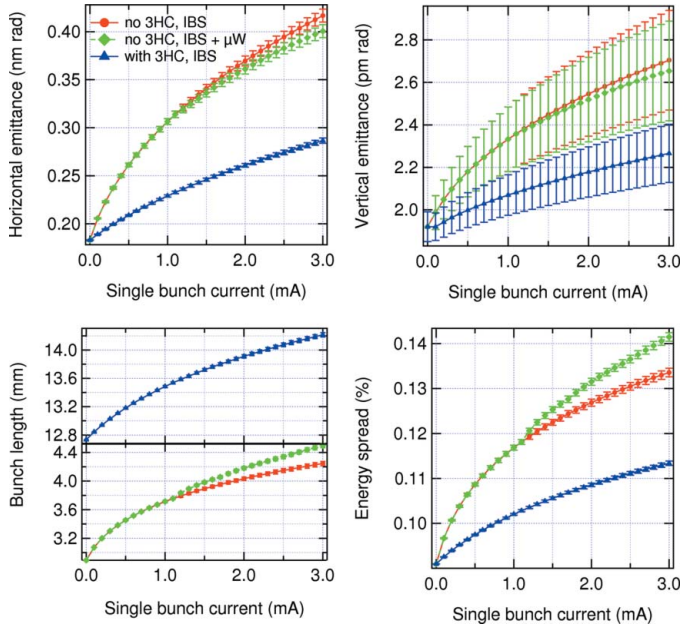

Figure 7
IBS and microwave instability effects calculated as a function of single-bunch current for Phase 2 with 3HC (triangles) and without 3HC (circles and diamonds). Top plots are horizontal and vertical emittances and lower plots are bunch length and energy spread. Red plots include IBS only and green ones also include microwave growth rate. Note that for the case with 3HC the longitudinal plane is stable due to the very long bunches.

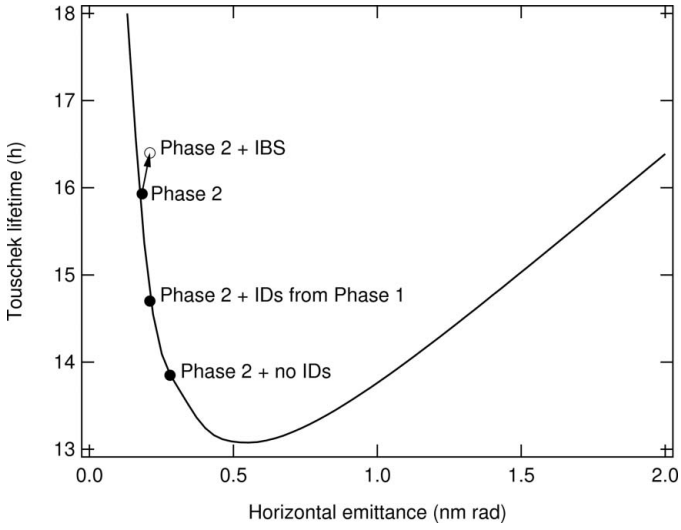

Figure 8
The trend line shows the Touschek lifetime for Phase 2, keeping all the other parameters constant. Full circles show the lifetime calculated using the natural horizontal emittance for the different scenarios. The arrow shows the changes from calculations without (filled circle) and with IBS effects (empty circle). While from the IBS effects the horizontal emittance growth leads to a reduction of the lifetime, the energy spread also increases, leading to a net increase in the Touschek lifetime.

feasible in the presence of challenging but achievable tolerances. The results for the optimized lattice show that top-up operation with conventional off-axis beam accumulation and beam lifetime larger than 10 h are possible. Operation at full current will require a harmonic cavity to lengthen the bunches. Instability thresholds and IBS effects have been estimated and are not expected to have a big impact on the Sirius performance parameters for uniform filling pattern. Hybrid filling mode limitations are still under study. The implementation of Sirius represents a challenge in terms of accelerator technology available today and, together with MAX IV, it will be an important step towards the next generation of hard X-ray diffraction-limited storage rings.

Table 6
Calculated partial and total beam lifetime for uniform fill and a single bunch in Sirius.

The calculations include IBS effects, 1% coupling and the parameters described in §3.

Scenario	$T_{elastic}$ (h)	$T_{inelastic}$ (h)	$T_{touschek}$ (h)	T_{total} (h)
Phase 0, commissioning	67.4	46.9	19.5	11.4
Phase 1	37.3	45.4	13.5	8.3
Phase 2	37.3	48.0	16.4	9.2
Phase 2, single-bunch 2 mA	37.3	48.0	5.2	4.2

The design of Sirius is a collective work that involves not only the entire LNLS team but also other colleagues from similar laboratories all over the world. We would like to thank everyone who has contributed in one way or another to the development of this project.

References

Borland, M. (2000). *elegant: A Flexible SDDS-Compliant Code for Accelerator Simulation, Presented at the 6th International Computational Accelerator Physics Conference, ICAP2000*, 11–14 September 2000, Darmstadt, Germany. Report No. LS-287.
Borland, M., Sajaev, V., Emery, L. & Xiao, A. (2010). Technical Report ANL/APS/LS-319. Advanced Photon Source, Argonne, IL, USA.
Cai, Y. (2011). SLAC Report PUB 14474. SLAC, Menlo Park, CA, USA.
Chin, Y. H. (1985). CERN Report CERN-SPS-85–2-(DI-MST). CERN, Geneva, Switzerland.
Chubar, O. & Elleaume, P. (1998). *Proceedings of EPAC98*, Stockholm, Sweden.
Leemann, S. C., Andersson, Å., Eriksson, M., Lindgren, L.-J., Wallén, E., Begtsson, J. & Streun, A. (2009). *Phys. Rev. ST Accel. Beams*, **12**, 120701.
Mounet, N. & Metral, E. (2009). Technical Report 039, CERN–BE Department, November 2009. CERN, Geneva, Switzerland.
Nagaoka, R. & Wrulich, A. (2007). *Nucl. Instrum. Methods Phys. Res. A*, **575**, 292–304.
Safranek, J., Portmann, G. & Terebilo, A. (2002). *Proceedings of EPAC 2002*, Paris, France.
Wang, C. (2009). *Phys. Rev. ST Accel. Beams*, **12**, 061001.